

# The Illumination of Thunderclouds by Lightning: Part 2: The Effect of GLM Instrument Threshold on Detection and Clustering

Michael Jay Peterson<sup>1</sup>, Tracy Ellen Lavezzi Light<sup>2</sup>, and Douglas Michael Mach<sup>3</sup>

<sup>1</sup>ISR-2, Los Alamos National Laboratory

<sup>2</sup>Los Alamos National Laboratory (DOE)

<sup>3</sup>Universities Space Research Association

November 26, 2022

## Abstract

Lightning is measured from space using optical instruments that detect transient changes in the illumination of the cloud top. How much of the flash (if any) is recorded by the instrument depends on the instrument detection threshold. NOAA's Geostationary Lightning Mapper (GLM) employs a dynamic threshold that varies across the imaging array and changes over time. This causes flashes in certain regions and at night to be recorded in greater detail than other flashes, and threshold inconsistencies will impose biases on all levels of GLM data products. In this study, we quantify the impact of the varying GLM threshold on event / group detection, flash clustering, and gridded product generation by imposing artificial thresholds on the event data taken from a thunderstorm with a low instrument threshold ( $\sim 0.7$  fJ). We find that even modest increases in threshold severely impact event (60% loss by 2 fJ, 90% loss by 10 fJ) and group (25% loss by 2 fJ, 81% loss by 10 fJ) detection by suppressing faint illumination of the cloud-top from weak sources and scattering. Flash detection is impacted less by threshold increases (4% loss by 2 fJ), but reductions are still significant at higher thresholds (35% loss by 10 fJ, or 44% if single-group flashes are removed). Undetected pulses cause individual flashes to be split and severely impact the construction of gridded products. All these factors complicate the interpretation of GLM data, particularly when trended over time under a changing threshold.

1                   **The Illumination of Thunderclouds by Lightning:**

2                   **Part 2: The Effect of GLM Instrument Threshold on Detection and Clustering**

3  
4                   **Michael Peterson<sup>1</sup>, Tracy E. L. Light<sup>1</sup>, Douglas Mach<sup>2</sup>**

5  
6                   <sup>1</sup>ISR-2, Los Alamos National Laboratory, Los Alamos, New Mexico

7                   <sup>2</sup>Science and Technology Institute, Universities Space Research Association,  
8                   Huntsville, AL, USA

9  
10  
11  
12  
13  
14 Corresponding author: Michael Peterson (mpeterson@lanl.gov), B241, P.O. Box 1663 Los  
15 Alamos, NM, 87545

16  
17  
18 **Key Points:**

- 19                   • GLM sensitivity is determined by the local threshold at each instrument pixel, which  
20                   varies across the imaging array and over time
- 21                   • High thresholds prevent detection of faint illumination, which limits the resolvable detail  
22                   of flashes or might prevent detection entirely
- 23                   • Instrument threshold affects all GLM products from event detections to flash clustering  
24                   and gridded product generation
- 25  
26  
27  
28

29 **Abstract**

30

31 Lightning is measured from space using optical instruments that detect transient changes  
32 in the illumination of the cloud top. How much of the flash (if any) is recorded by the instrument  
33 depends on the instrument detection threshold. NOAA's Geostationary Lightning Mapper  
34 (GLM) employs a dynamic threshold that varies across the imaging array and changes over time.  
35 This causes flashes in certain regions and at night to be recorded in greater detail than other  
36 flashes, and threshold inconsistencies will impose biases on all levels of GLM data products.

37 In this study, we quantify the impact of the varying GLM threshold on event / group  
38 detection, flash clustering, and gridded product generation by imposing artificial thresholds on  
39 the event data taken from a thunderstorm with a low instrument threshold ( $\sim 0.7$  fJ). We find that  
40 even modest increases in threshold severely impact event (60% loss by 2 fJ, 90% loss by 10 fJ)  
41 and group (25% loss by 2 fJ, 81% loss by 10 fJ) detection by suppressing faint illumination of  
42 the cloud-top from weak sources and scattering. Flash detection is impacted less by threshold  
43 increases (4% loss by 2 fJ), but reductions are still significant at higher thresholds (35% loss by  
44 10 fJ, or 44% if single-group flashes are removed). Undetected pulses cause individual flashes to  
45 be split and severely impact the construction of gridded products. All these factors complicate  
46 the interpretation of GLM data, particularly when trended over time under a changing threshold.

47

48

49 **Plain Language Summary**

50 Lightning is measured from space by optical instruments like the Geostationary  
51 Lightning Mapper (GLM). GLM detects rapid changes in cloud brightness from lightning  
52 illumination. How much of this illumination can be captured depends on the sensitivity of the  
53 instrument, which, for GLM, changes over space and time according to the local instrument  
54 threshold. At a low threshold - like we see at night or near the center of the GLM Field of View -  
55 flashes can be measured with a tremendous amount of detail. However, when the threshold is  
56 high – as it is during the day or in certain places like Colorado – only the brightest portions of a  
57 flash might be seen, if the flash is detected at all.

58 In this study, we characterize the effect of the GLM instrument threshold on each type of  
59 GLM data. We find that removing faint detections by imposing higher thresholds affects every  
60 type of GLM data. These results demonstrate that situational context is important for evaluating  
61 GLM data – particularly when trended over time under a changing threshold.

62

## 63 **1 Introduction**

64

65 Cloud-to-Ground (CG) strokes detected by optical or Radio Frequency (RF) sensors are  
66 only a small part of the larger lightning “tree” that extends throughout the cloud. Lightning  
67 activity includes a variety of CG and in-cloud phenomena that radiate across a vast range of  
68 energies and frequencies. What parts of the flash that are resolved depends on the sensitivity of  
69 the instrument and the portion of the electromagnetic spectrum it measures. Both VHF-band  
70 Radio Frequency (RF) instruments and optical sensors are capable of mapping major portions of  
71 the lightning tree (Rison et al., 1999; Peterson et al., 2018) and detecting powerful emissions  
72 from strokes (Light et al., 2001a; Koshak, 2010). RF or optical sensors with low sensitivities  
73 may only detect the particularly-energetic strokes or similarly-powerful in-cloud events  
74 (Jacobson and Light, 2011), while the most sensitive instruments will be able to map nearly the  
75 full extent of the lightning tree – which can cover hundreds of kilometers (Lang et al., 2017;  
76 Peterson et al., 2020).

77 Optical sensors have the additional issue that the lightning emissions – regardless of  
78 power – will be significantly modified by absorption and scattering in the cloud medium between  
79 the source and satellite (Thomson and Krider, 1982; Koshak et al., 1994; Light et al., 2001b;  
80 Brunner and Bitzer, 2020; Peterson, 2020a). Cloud regions that are particularly opaque to  
81 lightning signals (either from large optical depths or a composition / geometry that favors diffuse  
82 reflection off cloud sides over transmission through the medium) can prevent the detection of  
83 even powerful optical lightning signals from space – which we can be seen as anomalies in the  
84 radiance data (Peterson, 2020b). Opaque clouds lead to poor Detection Efficiencies (DEs) for  
85 instruments like the Geostationary Lightning Mapper (GLM: Goodman et al., 2013; Rudlosky et

86 al., 2019) in certain types of storms with problematic precipitation structures (Bitzer, 2019; Said  
87 and Murphy, 2019; Thomas, 2019; Rutledge et al., 2019).

88         The attenuation of the optical lightning signals by the cloud medium suggests that optical  
89 space-based lightning detectors have more to gain from optimizing for sensitivity compared to  
90 other types of instruments – for examples, RF detectors. Scattering is particularly problematic for  
91 pixelated optical detectors compared to sensitive photodiode detectors, as the dispersed signal  
92 may be divided between pixels. This likely contributes to discrepancies between instruments  
93 noted in van der Velde and Montoya (2020). Any improvements in sensitivity from lowering the  
94 detection threshold will allow the instrument to recover flashes that are obscured below optically  
95 thick clouds, while also resolving more of the lightning tree in all flashes. The primary concern  
96 in lowering the threshold is a dramatic increase in solar artifacts (Peterson, 2020c) and noise  
97 events. However, the potential benefits of such an optimized threshold for GLM’s diverse  
98 collection of operational products have not been fully quantified.

99         The GLM threshold affects not only how much of the flash can be detected from space, it  
100 also limits the amount of thundercloud illumination that is measured from orbit. Scattering  
101 interactions allow optical lightning sources to illuminate the cloud scene far beyond the extent of  
102 the lightning tree. The most powerful groups detected by the Lightning Imaging Sensor (LIS:  
103 Christian et al., 2000; Blakeslee et al., 2020) and GLM encompass 10,000+ km<sup>2</sup> of the cloud-top  
104 (Peterson et al., 2017) – and include large areas of lower clouds that can transmit low-altitude  
105 lightning emissions or reflect high-altitude lightning emissions to provide a “shortcut” path to the  
106 satellite compared to traversing the full optical depth of convective cloud (Peterson, 2019a;  
107 Peterson et al., 2020b). Much of this neighboring cloud illumination is sufficiently dim to  
108 quickly fall below higher thresholds.

109           This is the second part of our thundercloud illumination study. In Part 1 (Peterson et al.,  
110 2021a), we examined how the positions and geometries of optical sources affected GLM  
111 measurements of cloud illumination. In Part 2, we shift our focus from the emitter to the GLM  
112 instrument and quantify the effects of the GLM threshold on event / group detection, flash  
113 clustering, and gridded product generation. We take the Colombia thunderstorm from Part 1 that  
114 had a low GLM threshold of  $\sim 0.7$  fJ, impose artificial thresholds on the event data between 1 fJ  
115 and 10 fJ, and then recompute the GLM cluster feature and gridded products using only the  
116 events above the imposed threshold. Changes in lightning rates and flash characteristics are  
117 discussed, along with how these changes affect the products downstream.

118

## 119 **2 Data and Methodology**

120           This study will use the matched GLM and LMA data from Part 1 that describes lightning  
121 activity in two thunderstorms (one in Colombia and the other in Colorado) to examine the effect  
122 of the GLM threshold on each type of GLM data product. The primary focus will be on the  
123 Colombia thunderstorm that was close to the GOES-16 satellite subpoint and had a low overall  
124 instrument threshold. With this low threshold, we can impose artificial event energy thresholds  
125 on the GLM data to determine how higher thresholds would impact detection, clustering, and  
126 gridded product generation for the same thunderstorm. Data from the Colorado thunderstorm  
127 will also be shown, but only as a point of reference for an observed case with a high threshold.

### 128 *2.1 The GOES-16 Geostationary Lightning Mapper*

129           GLM is a staring imager that records cloud-top illumination in a narrow spectral band  
130 around the 777.4 nm Oxygen emission line triplet at 500 frames per second (Goodman et al.,

131 2013). Transient changes in cloud-top illumination characteristic of lightning are detected by  
132 subtracting the estimated background brightness of a given pixel from the pixel energy recorded  
133 during a 2-ms integration frame, and then comparing the remaining signal energy with the  
134 current local instrument threshold. If the recorded energy is greater than the threshold, the  
135 instrument will trigger and report an event at that pixel. These pixel events are then clustered into  
136 higher-level features that describe lightning - including “groups” (which approximate lightning  
137 pulses) and flashes (Goodman et al., 2010; Mach, 2020). This cluster data is then used to  
138 construct GLM gridded products such as Flash Extent Density (FED), Average Flash Area  
139 (AFA), and Total Optical Energy (TOE) (Bruning et al., 2019).

140         The GLM data produced and distributed by NOAA, however, is subject to the limitations  
141 in the Lightning Cluster Filter Algorithm (LCFA: Goodman et al., 2010), which must run in an  
142 operational setting with strict latency requirements. To ensure timely data, the LCFA imposes  
143 arbitrary limits on group and flash clusters that prevent them from becoming too large or  
144 complex. These thresholds (101 events per group, 101 groups per flash, and a maximum flash  
145 duration of 3 s) are rather low compared to even LIS flashes (Peterson et al., 2017), and cause  
146 the most exceptional cases of lightning (i.e., Peterson et al., 2020a) to be artificially split into  
147 multiple pieces that are flagged as a “degraded” quality in the operational GLM data. To recover  
148 these flashes, Peterson (2019) developed methods that can be applied in post-processing to repair  
149 the flash cluster data and generate science-quality GLM data. This data is available at Peterson  
150 (2021a). As in Part 1, we use the repaired data here rather than the operational LCFA data.

151         *2.2 Approximating GLM Thresholds and Imposing Artificial Thresholds*

152           While the threshold at each pixel is not specified for GLM events, threshold values can  
153 be estimated from the lowest-energy events reported by GLM (Figure 1a in Peterson and Lay,  
154 2019). If GLM can detect events from a thunderstorm down to 1 fJ, then the threshold must be  
155 somewhere below (and probably close to) 1 fJ – otherwise dimmer events would be reported.  
156 These estimates allow us to examine relative differences in threshold from storm to storm and  
157 from region to region, and to trend thresholds over time. However, minimum event energy is not  
158 a perfect approximation to the threshold at the pixel level. Radiative transfer across the cloud  
159 scene affects the energy distribution of recorded events. For example, cloud regions that do not  
160 produce lightning still can be illuminated by very bright lightning pulses from a nearby  
161 thunderstorm (i.e., Peterson et al., 2017). If these are the only optical pulses that generate GLM  
162 events in a particular pixel, then the minimum reported energy will be quite high compared to  
163 pixels in the nearby thunderstorm core. In the storm core, meanwhile, at least some of the  
164 lightning pulses will be rather dim, producing events near the actual threshold.

165           In the absence of an optical phenomenon that is known to significantly raise the local  
166 GLM threshold (an example being sustained illumination from solar glint: Peterson, 2020c), the  
167 actual threshold should not be substantially different between neighboring cloud regions that are  
168 subject to the same background illumination. Thus, the minimum event energies over a flash- or  
169 convective-scale region are expected to be a better approximation for the nominal threshold  
170 throughout that region than the minimum energies reported at each pixel. We use the flash  
171 minimum event energy per flash as our threshold proxy in this study.

172           Artificial thresholds above the local instrument threshold are applied to the GLM  
173 detections by collecting all the event data from the Colombia thunderstorm, removing detections  
174 that are less energetic than the chosen artificial threshold, and then reconstructing the derived

175 GLM data products from the events that exceed the new threshold (for example, the  
176 meteorological imagery in Bruning et al., 2019). We consider artificial thresholds between 1 fJ  
177 and 10 fJ in this study, which correspond to typical GLM thresholds over the regions across the  
178 Americas where lightning is most common (i.e., Figure 1 in Rudlosky et al., 2019; Figure 5 in  
179 Peterson, 2019). Higher minimum event energy values are found at the edge of the instrument  
180 FOV, but these likely result from biases in the pixel energy distributions from the near side-view  
181 of thunderstorms in these regions rather than the true local instrument threshold. Thus, higher  
182 thresholds will not be considered.

183         The removal of dim events and groups under higher thresholds can cause single flashes to  
184 become split if the remaining groups / events no longer meet the LCFA clustering criteria. While  
185 higher thresholds reduce the number of flashes detected by GLM, flash splitting artificially  
186 increases the number of flashes that would be detected. As these split flashes do not represent  
187 physically distinct features, we examine the effect of this splitting separately from the loss of  
188 GLM detections. Section 3.2 examines the consequences of event / group / flash losses under  
189 each threshold using the original cluster data that best captures the physical development of each  
190 flash. Then, Section 3.3 examines how flash splitting modifies these results by constructing new  
191 cluster data using the remaining events at each artificial threshold.

192

### 193 **3 Results**

#### 194 *3.1 GLM Thresholds in Colorado and Colombia Thunderstorms*

195         GLM is known to have a relatively high threshold in parts of Colorado. To test this  
196 assertion and quantify differences in threshold between the Colorado and Colombia

197 thunderstorms, we construct timeseries of minimum GLM event energies in Figure 1 for the  
198 Colombia (Figure 1a) and Colorado (Figure 1b) thunderstorms. As in the timeseries in Figure 1  
199 (Colombia) and Figure 3 (Colorado) in Part 1, times are relative to 00:00 UTC on the first day of  
200 the storm (11/1/2019 for Colorado and 7/1/2019 in Colorado), and only GLM lightning activity  
201 in the LMA data domain (defined by latitude and longitude boxes) are shown. The red timeseries  
202 in Figure 1 show the minimum GLM event energy for any pixel within the LMA data domain,  
203 while the dark blue timeseries averages the minimum event energies across all pixels with  
204 lightning in the domain, and the light blue timeseries shows the maximum value of minimum  
205 event energy in any pixel. Horizontal lines are drawn to show constant energies from 1-5 fJ  
206 (solid) as well as 10 and 100 fJ (dashed).

207         We noted in Part 1 that there were periods of time during the Colorado storm where  
208 lightning activity occurred in the warmer clouds surrounding deep convection, but not in the  
209 thicker convective clouds, themselves. This indicates that the sample of lightning measured by  
210 GLM will be biased towards the brighter flashes and the minimum pixel energy in these  
211 peripheral regions is not expected to be the best representation of the actual GLM threshold.  
212 Throughout the timeseries in Figure 1b, the lowest event energies (red) range from <1 fJ to  
213 nearly 5 fJ, while the maximum pixel values of minimum event energy reach 70 fJ - causing  
214 average pixel values to range from 5 to 10 fJ. The minimum event energy also varies according  
215 to time of day, with the red curve starting at 5 fJ in the late afternoon and largely decreasing  
216 below 2 fJ after nightfall. Examining changes in flash count and Total Optical Energy (TOE)  
217 after imposing artificial thresholds between 1 fJ and 10 fJ (not shown for the Colorado case)  
218 indicates that the overall effective threshold for the Colorado thunderstorm was between 3 and 4  
219 fJ, as this is the point where notable changes in the GLM detection totals begin to occur.

220           Thresholds in the 3-4 fJ range are still relatively high for GLM. The Colombia case  
221 (Figure 1a) is expected to have a low threshold due to its proximity to the satellite subpoint.  
222 Indeed, the lowest event energies (red curve) during the most active storm period (6-11 UTC) are  
223 universally below 1 fJ. As before, certain pixels have greater minimum event energy values  
224 (light blue curve) up to 30 fJ, and these impact the overall domain mean (blue curve). However,  
225 the overall effective GLM threshold for the region is inferred to be  $< 1$  fJ, and probably close to  
226 the  $\sim 0.7$  fJ average for the red curve during this period.

227

### 228           3.2 *The effect of GLM Threshold on Event / Group / Flash Detection*

229           Artificial thresholds of between 1 fJ and 10 fJ are imposed on the GLM event data from  
230 the Colombia thunderstorm to determine how many of the original flashes are removed by  
231 increasing the threshold. Figure 2 shows how event count (a), group count (b), flash count (c),  
232 and TOE (d) change under each imposed threshold. Solid lines include all the GLM data, while  
233 the dashed lines do not consider data from single-group flashes that are removed by the current  
234 version of the LCFA (Rudlosky and Virts, 2021). As minimum event energy values were close to  
235 1 fJ in Figure 2e, there is little difference between no imposed threshold (0 fJ) and a 1 fJ  
236 threshold in any of the plots. However, increasing the threshold just to 2 fJ severely impacts  
237 event detection (Figure 2a). By a 4 fJ threshold (comparable to the Colorado case), 70% of the  
238 original events have been eliminated, while 90% of events are missed under a 10 fJ threshold.

239           The loss of these dim events under higher thresholds affects group and flash detection,  
240 TOE, and the characteristics of the remaining groups and flashes. Overall group counts (Figure  
241 2b) are reduced by 25% under a 2 fJ threshold, 55% by 4 fJ, and 81% by 10 fJ. TOE (Figure 2d),  
242 meanwhile, is reduced by 12% by 2 fJ, 29% by 4 fJ, and 53% by 10 fJ. The TOE values in

243 Figure 2d accumulate all events from the Colombia thunderstorm, but TOE is also reported as a  
244 gridded product. The severe losses in TOE at the storm level between a 1 fJ and 10 fJ threshold  
245 are the first indication that changing thresholds will become important when trending GLM  
246 grids.

247         Of the four parameters considered in Figure 2, flash count (Figure 2c) is the key metric  
248 for GLM performance, and it is least impacted by thresholds changes. Only 4% of the original  
249 flashes (solid line) are lost by increasing the threshold to 2 fJ, 15% by 4 fJ, and 35% by 10 fJ.  
250 Many of these flashes are reduced to a single group, however, and would not be reported by the  
251 LCFA. Removing these flashes (dashed line) increases the overall losses to 7% by 2 fJ, 20% by 4  
252 fJ, and 44% by 10 fJ. Still, these losses are small compared to the total event and group counts  
253 and thunderstorm TOE values in Figure 2, suggesting that the primary effect of an increased  
254 threshold is the loss of the flash detail and the extent of cloud illumination that can be resolved.

255         Figure 3 shows the remaining groups that do not fall completely below threshold and  
256 plots histograms of group energy (Figure 3a) and group footprint area (Figure 3b) (as a percent  
257 of the original group area / energy) under thresholds ranging from 1 fJ to 10 fJ. For each  
258 threshold, the horizontal bins in Figure 3 sum to 100%. Percentiles are also tracked between  
259 thresholds with line overlays. While these groups are still resolved by GLM, their appearance is  
260 significantly modified under the increased thresholds. The median group energy declines to two-  
261 thirds of the energy of the original group, while the median group area is reduced to one-fourth  
262 of the original group area. However, not all groups are affected in the same way, leading to a  
263 broad range of possible energy reductions under higher thresholds. While some groups lose  
264 virtually none of their original energy by 10 fJ, others lose 95%.

265         The group area distributions in Figure 3b show that the loss of faint events at higher

266 thresholds causes the group area to be substantially eroded. While quantization from an integer  
267 number of illuminated pixels limits the possible values and causes percentages that correspond to  
268 rational numbers (i.e., 25%, 50%) to stand out, the distributions still show that group area is  
269 more sensitive to threshold effects than group energy. This is because most of the events that  
270 comprise a group are rather dim compared to the brightest event in the group. A point source  
271 within a cloud may consist of a single bright event in the pixel over the source with a  
272 surrounding ring of dim events. In this case, there will be one brighter event, and then eight dim  
273 events in the ring. Thus, the dim pixels in a group will far outnumber the bright pixels. Even  
274 increasing the threshold slightly to 2 or 3 fJ severely impacts the detection of peripheral dim  
275 events, and the median group area is reduced by half while the median group energy only  
276 declines by 12%. Under the highest thresholds, groups might only contain the single brightest  
277 event.

278 To determine what this event loss does to flash characteristics, Figure 4 repeats the  
279 analysis from Figure 3 at the flash level. Flashes must have at least one event above the  
280 maximum threshold (10 fJ) to be considered, and all groups that fall below the threshold will not  
281 contribute to the flash energy (Figure 4a) or flash area (Figure 4b). The key difference between  
282 the group level (Figure 3) and the flash level (Figure 4) characteristics is the notable lack of  
283 flashes that are virtually unchanged from the original threshold. Even moderate thresholds of 2-3  
284 fJ are sufficient to erode much of the flash energy and at least some of the flash area.

285 The reductions in flash energy are more severe than group energy losses because flashes  
286 are comprised mostly of small dim groups offset by a few bright pulses (Peterson et al., 2018).  
287 While individually dim, the total energy from these pulses has a significant impact on the overall  
288 flash energy - and they are removed entirely under these higher thresholds alongside the dim

289 portions of the brighter groups. The flash area reductions, meanwhile, are comparable to the  
290 group area reductions that we saw previously in Figure 3. This is probably not a coincidence, as  
291 flash area is often determined by the largest group in the flash (Peterson et al., 2017). Lateral  
292 propagation only plays a central role in determining flash area once the group separation exceeds  
293 the scale of these brighter individual GLM groups.

294

### 295 *3.3 The effect of GLM Threshold on Flash Clustering*

296 The complete loss of dim groups and erosion of brighter groups under an increased  
297 threshold poses a challenge for GLM lightning mapping and flash clustering. Flash structure is  
298 mapped by tracking the faint localized discharges that occur along the developing branches of  
299 the flash. As these events fall below threshold, the GLM maps resolve flash structure using an  
300 increasingly-smaller number of points – adding uncertainty to the path that was taken by the  
301 flash through the cloud. Eventually, the removal of these dim events will reach a point where the  
302 remaining events become separated in space and time beyond the thresholds used by the GLM  
303 clustering algorithm (Goodman et al., 2010). This causes the original single lightning flash to be  
304 split into multiple flash features that represent different illuminated portions of the lightning tree.

305 Figure 5 demonstrates how increasing the threshold affects clustering using the case of a  
306 long horizontal lightning flash from the Colombia thunderstorm. The flash is mapped with a  
307 color contour representing the TOE from only the flash in question, and with a line segment  
308 overlay connecting subsequent groups in the flash. If the original flash becomes split into  
309 multiple flash features, each of these split flashes will be assigned a different color for the group  
310 line segment overlay. Index numbers for each split flash are also drawn in its assigned color. The  
311 flash is plotted under the original threshold in Figure 5a. Most of the group activity in the flash

312 occurred along its southern flank, while a linear branch can also be noted extending to the  
313 northeast. TOE values were reasonably-high over most of the flash footprint (i.e., > 100 fJ) - but  
314 note that these are summed over all events, which can mask large numbers of events that are  
315 removed under the higher thresholds.

316         Figure 5b removes all events below a 3 fJ threshold and then reclusters the flash using the  
317 remaining events. While the flash extent is reduced under this higher threshold due to the loss of  
318 groups at the ends of the southern and northeastern branches, the overall flash structure is mostly  
319 intact. However, the large distance between some of the groups (i.e., long straight lines in Figure  
320 5b) - particularly along the northern branch - signify that the group separations are approaching  
321 the limits of the clustering algorithm (16.5 km, 330 ms). The clustering algorithm still clusters  
322 these groups into a single flash at this point because GLM clustering depends on the separation  
323 of events within a group and not the separations of group centroids that are depicted by the line  
324 segments. Still, the large group spacing indicates that we have limited information about how the  
325 northern branch of the flash developed, and further increasing the threshold is likely to result in  
326 splitting.

327         Figure 5c increases the threshold up to 6 fJ, causing in the first split section from the  
328 original flash. Removing the events below this threshold prevents most of the development of the  
329 northern branch from being resolved. The branch is still evident as a contiguous feature in the  
330 TOE plot, but the individual groups that would be detected by GLM are too far apart in space  
331 and time to meet the GLM definition of a flash. Thus, the collection of groups at the far end of  
332 the branch are split into a distinct flash feature (depicted with blue line segments and assigned an  
333 index of 2) from the primary flash (colored black with the original index of 1). Continuing to  
334 increase the threshold to 9 fJ (Figure 6d) splits the northern branch of the flash further into a

335 third central piece (colored red with an index of 3). Thus, we have the primary flash (black), the  
336 larger central split flash (red) and the original split flash at the end of the branch (blue) – which  
337 has been reduced to a single point and would not be reported by the current version of the LCFA,  
338 as it filters out these single-group flashes.

339 Flash splitting artificially increases thunderstorm flash counts. Long horizontal flashes  
340 like the case in Figure 5 are particularly problematic because their lateral development makes  
341 them prone to being broken into multiple small pieces (as we saw in Figure 5d) rather than two  
342 roughly equal sized pieces. Moreover, as these flashes occur outside of the convective core  
343 where flash rates are generally low to begin with, any splitting will noticeably alter the local flash  
344 rate. The scale of this problem is demonstrated in Figure 6 by quantifying flash splitting  
345 frequency at each flash size and imposed threshold. Flash splitting is not a severe issue for  
346 convective-scale flashes (i.e., ~10 km in size), as < 10% of flashes are split at any threshold.  
347 However, when flashes grow to 50-km, more than half are split at the higher thresholds (i.e., >3  
348 fJ) and nearly 80% of the largest flashes (100+ km) at the highest thresholds (5-10 fJ) are split.

349 It is not immediately clear how much the threshold-based splitting will change the overall  
350 flash rate for a given thunderstorm because the larger flashes that are frequently split are far less  
351 common than the convective-scale flashes that remain intact at higher thresholds. To assess the  
352 impact of splitting on the flash rates from the Colombia thunderstorm, Figure 7a counts the  
353 number of reclustered flashes at each threshold and compares this number to the original flash  
354 counts from Figure 2c. As before, we consider both the case of all flashes (solid lines) and multi-  
355 group flashes (dashed lines) that are not removed by the current LCFA. When the imposed  
356 threshold is near the instrument threshold (i.e., 0 fJ – 1 fJ), the original (black curves) and  
357 reclustered (blue curves) flash counts are nearly identical. However, imposing a 2 fJ or higher

358 threshold causes the reclustered curves to increase beyond the original flash count curves. All the  
 359 curves in Figure 7a decrease at higher thresholds as whole flashes fall below the threshold, but  
 360 the separation in the curves remains fairly constant. Figure 7b quantifies this by computing the  
 361 ratios between the reclustered flash counts and the original flash counts at each threshold. Flash  
 362 splitting artificially increases the overall flash rate from the Colombia thunderstorm by 6% for all  
 363 flashes and 3% for multi-group flashes under a 2 fJ threshold, 9% and 6% under a 4 fJ threshold,  
 364 and 12% and 7% under a 10 fJ threshold. These increases partially counteract the 35% (all  
 365 flashes) and 44% (multi-group flashes) loss in flash count over the same threshold range that we  
 366 described in Figure 2c, but these apparent improvements in the detected flash rates are only the  
 367 result of artificial biases in the GLM data.

368

### 369 *3.4 The effect of GLM Threshold on Gridded Product Generation*

370 The GLM threshold affects the gridded products generated from flash cluster data by  
 371 combing the effects discussed in the previous sections. These include:

- 372 (1) Removing below-threshold events at the periphery of the flash / group footprints  
 373 reduces the spatial extent of features in the gridded data.
- 374 (2) Eliminating below-threshold events modifies the flash characteristics represented in  
 375 the grids – both in the original sample of flashes, and following the threshold-based  
 376 artificial flash splitting.
- 377 (3) Removing below-threshold events / groups / flashes modifies the sample of lightning  
 378 used to generate the grids - introducing a bias towards the more prominent flashes  
 379 that can survive the removal of below-threshold events (including the LCFA removal  
 380 of single-group flashes).

381 While the degree to which the above effects impact the GLM gridded products differs  
382 from grid to grid, it generally depends on whether the grid is generated by summing / averaging  
383 flash characteristics (i.e., TOE, FED, AFA, Average Flash Extent, Average Flash Duration) or by  
384 looking at their minimum values (i.e., Minimum Flash Area: MFA). Grids based on maximum  
385 flash characteristics are not considered here but would more closely resemble the total / mean  
386 grids than the minimum grids. We elect to discuss two representative grids that demonstrate  
387 these effects – AFA and MFA – and provide the remaining grids as Supporting Information. All  
388 of these grids are generated using only multi-group flashes that would not be removed by the  
389 LCFA.

390 AFA grids are shown in Figure 8 for imposed thresholds between 0 fJ and 10 fJ, with an  
391 increment of 2 fJ between panels. Note that an exponential scale is used to capture the large  
392 dynamic range of GLM flash areas, so even slight changes in color represent a notable difference  
393 in flash size. When no artificial threshold is imposed, flash sizes within the primary storm feature  
394 at the center of the image range from 600 km<sup>2</sup> at its center to over 5,000 km<sup>2</sup> at its northwest  
395 edge. This behavior is largely due flashes of all energies illuminating the convective core of the  
396 thunderstorm while the brightest flashes can also illuminate neighboring clouds - but long  
397 horizontal flashes can also contribute to larger flash areas in these non-convective regions.

398 Imposing a threshold of even 2 fJ (Figure 8b) removes much of the illumination around  
399 the edge of the thunderstorm feature, while causing all AFA values to decrease. The largest AFA  
400 values are around 3000 km<sup>2</sup> while the convective core sees its first pixels in the 300-600 km<sup>2</sup>  
401 range. Increasing the threshold further from 4 fJ up to 10 fJ (Figure 9c-f) continues these trends:  
402 the thunderstorm feature becomes smaller while the AFA values continue to decline. What was  
403 initially a region of small flashes surrounded by larger flash areas under a < 1 fJ threshold is

404 reduced to a cluster of small flashes by 10 fJ with only a few pixels of increased flash areas on  
405 the northwestern flank to indicate the larger flash areas from the original grid.

406         These changes in AFA are modest compared to grids that examine minimum values like  
407 MFA. Figure 9 shows the MFA grids at each threshold level during the same thunderstorm  
408 snapshot as Figure 8. Removing dim GLM events has greater effect on MFA because only the  
409 brightest events in the groups that comprise a given flash might exceed the imposed threshold.  
410 Thus, while the initial MFA grid in Figure 9a might resemble an amplified version of the AFA  
411 grid in Figure 8 that emphasizes the small flashes in the convective core and the larger flashes  
412 that illumine its periphery, minimum flash sizes quickly fall off across the thunderstorm feature  
413 as thresholds are increased beyond 2 fJ (Figure 9c-f). By a 10 fJ threshold, nearly half of the  
414 gridpoints within the feature correspond to flashes consisting of only 1-pixel GLM flashes, and  
415 the remainder are  $< 200 \text{ km}^2$  in size.

416         These variations in AFA and MFA with threshold demonstrate the challenge of trending  
417 GLM gridded products over time. Thresholds usually change from day to night and, as we saw in  
418 Figure 1b for the Colorado case, these changes can extend over multiple femtojoules of event  
419 energy. This is further complicated by threshold differences across the GLM imaging array (i.e.,  
420 between RTEPs). As storms move and develop over time, the characteristics of their flashes will  
421 change, driving trends in the GLM gridded products. But these trends will be confounded by any  
422 changes in threshold that occur over the same period. To mitigate threshold biases in gridded  
423 product trends, it is necessary to construct grids that remain consistent over the life cycle of the  
424 storm in question. Imposing artificial thresholds at the highest threshold values encountered by  
425 the storm of interest, as we have done here, is one way of doing this. However, this comes with  
426 the cost of losing much of the flash detail that is required to measure the flash characteristics

427 being trended.

428

#### 429 **4 Conclusion**

430 This second part of our thundercloud illumination study focuses on the effect that the  
431 GLM instrument threshold has on GLM data products. To quantify threshold effects, we  
432 consider a thunderstorm that occurred with a low instrument threshold ( $\sim 0.7$  fJ), impose artificial  
433 thresholds over the range of 1 fJ to 10 fJ, and then examine how each type of GLM data product  
434 is modified by these threshold changes.

435 The primary effect of the threshold-based changes to the GLM products is the loss of  
436 faint events that are present under lower thresholds. Losing the below-threshold dim events  
437 erodes the footprints of GLM groups and flashes until they fall completely below the higher  
438 threshold and go undetected. As flashes are comprised primarily of dim events and groups offset  
439 by a few energetic pulses, increasing the instrument threshold has a greater impact on event and  
440 group detection than on flash detection. Imposing a 2 fJ artificial threshold on our thunderstorm  
441 case decreases the event count by 60% compared to the original data, while imposing a 10 fJ  
442 threshold removes 90% of the original events. Meanwhile, 25% of groups are removed with a 2  
443 fJ threshold and 81% are lost under a 10 fJ threshold.

444 The threshold effect on flash detection is complicated by losing dim events and groups  
445 that can result in flash splitting as the remaining events and groups exceed the space and time  
446 thresholds employed by the GLM clustering algorithm. Of the original GLM flashes, 4% fall  
447 completely below a 2 fJ threshold and 35% are eliminated by a 10 fJ threshold. The current  
448 version of the GLM LCFA also removes single-group flashes. Filtering out these flashes

449 increases the threshold-induced losses to 7% by 2 fJ, 20% by 4 fJ, and 44% by 10 fJ. At the same  
450 time, flash splitting artificially increases the overall flash count by 6% at 2 fJ and up to 12% by  
451 10 fJ and the multi-group flash count by 3% at 2 fJ and up to 9% by 10 fJ.

452         Gridded products generated from GLM flash cluster data are also severely impacted by a  
453 combination of missed / split flashes and reductions in the flash / group footprints at higher  
454 thresholds. We consider the AFA and MFA products as representative of total / mean /  
455 maximum products (AFA) and minimum products (MFA) and examine how they change  
456 under the imposed thresholds. The size of the GLM feature describing the illuminated  
457 thunderstorm decreased under higher thresholds, as illumination around the periphery of the  
458 storm core from distant bright / large flashes quickly falls below threshold. Flash sizes within the  
459 storm core also generally decreased due to smaller flashes losing portions of their footprints, and  
460 flash splitting. The key difference between AFA and MFA is the scale of this reduction in area.  
461 As MFA examines the minimum flash area, flashes comprised of a few events just above the  
462 threshold can report flash areas corresponding to just 1 or 2 GLM pixels. This is problematic for  
463 non-convective storm regions that produce large lightning flashes, as these long horizontal  
464 flashes are more prone to splitting at higher thresholds than small convective-scale flashes.

465         These results demonstrate the importance of considering the context surrounding GLM  
466 detections – the configuration of the cloud scene, corresponding instrument threshold, location,  
467 and time of day, etc. - when interpreting GLM data. This is particularly important when  
468 accumulating data from a diverse collection of lightning flashes (for example, when generating  
469 gridded products) or trending GLM data over time. Changes in the situational context (for  
470 example, spatial / diurnal changes in threshold) can have a considerable impact on the results.

471 Future work in Part 3 (Peterson et al., 2021b), will leverage these results to show how  
472 the altitude of the source within the cloud can be estimated from group-level cloud illumination  
473 metrics. Finally, Part 4 (Peterson et al., 2021d) will evaluate volumetric meteorological and  
474 thundercloud imagery derived from GLM data.

475

## 476 **Acknowledgments**

477 This work was supported by the US Department of Energy through the Los Alamos National  
478 Laboratory (LANL) Laboratory Directed Research and Development (LDRD) program under  
479 project number 20200529ECR. Los Alamos National Laboratory is operated by Triad National  
480 Security, LLC, for the National Nuclear Security Administration of U.S. Department of Energy  
481 (Contract No. 89233218CNA000001). The work by co-author Douglas Mach was supported by  
482 ASA 80MFSC17M0022 “Cooperative Agreement with Universities Space Research  
483 Association” and NASA Research Opportunities in Space and Earth Science grant  
484 NNX17AJ10G “U.S. and European Geostationary Lightning Sensor Cross-Validation Study.”  
485 We would like to thank the operators of the Colorado LMA at Colorado State University and the  
486 Colombia LMA at the Technical University of Catalonia, and Drs. Ken Cummins and Jesús  
487 López for sharing their processed LMA data for the presented cases. The data used in this study  
488 is available at Peterson (2021b).

## 489 **References**

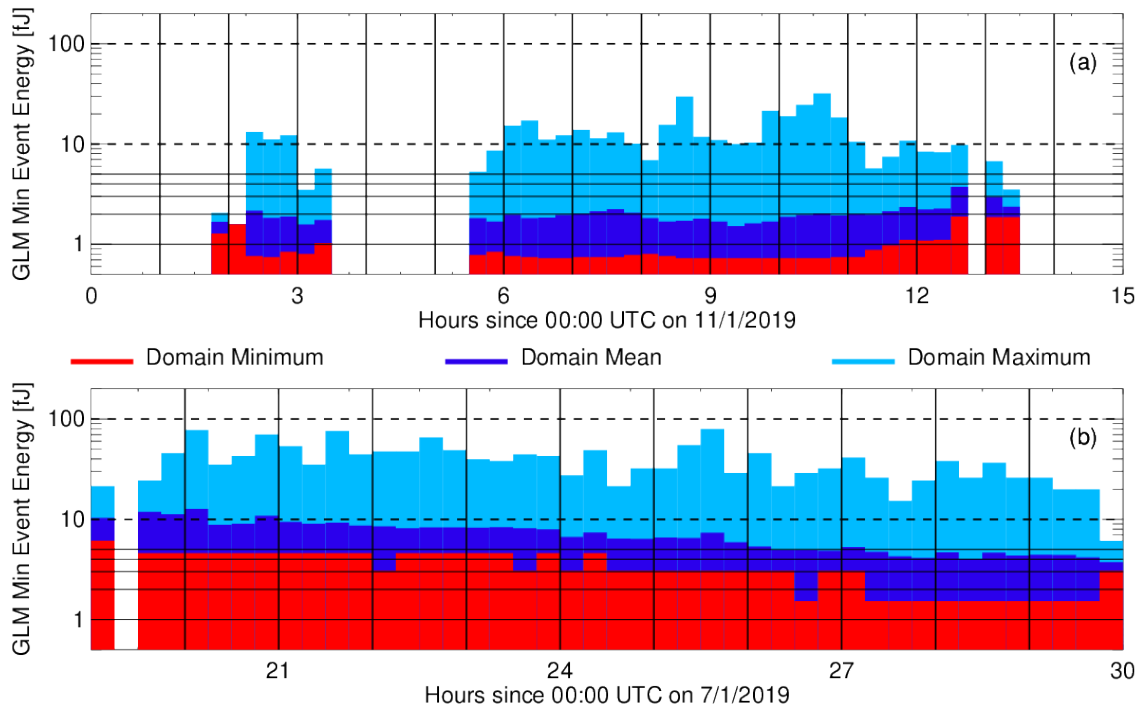
490  
491 Bitzer, P. M., (2019). The fruit basket of GLM detection efficiency. *GLM Science Team*  
492 *Meeting, 2019*. Huntsville, AL, USA, 33 slides. Available online at: [https://goes-](https://goes-r.nsstc.nasa.gov/home/sites/default/files/2019-09/Bitzer_20190912_glm_sci_mtg.pptx)  
493 [r.nsstc.nasa.gov/home/sites/default/files/2019-09/Bitzer\\_20190912\\_glm\\_sci\\_mtg.pptx](https://goes-r.nsstc.nasa.gov/home/sites/default/files/2019-09/Bitzer_20190912_glm_sci_mtg.pptx).

- 494 Blakeslee, R.J., Lang, T.J., Koshak, W.J., Buechler, D., Gatlin, P., Mach, D.M., Stano, G.T.,  
495 Virts, K.S., Walker, T.D., Cecil, D.J., Ellett, W., Goodman, S.J., Harrison, S., Hawkins,  
496 D.L., Heumesser, M., Lin, H., Maskey, M., Schultz, C.J., Stewart, M., Bateman, M.,  
497 Chanrion, O. and Christian, H. (2020), Three Years of the Lightning Imaging Sensor  
498 Onboard the International Space Station: Expanded Global Coverage and Enhanced  
499 Applications. *J. Geophys. Res. Atmos.*, **125**: e2020JD032918.  
500 <https://doi.org/10.1029/2020JD032918>
- 501 Brunner K., & P. M. Bitzer (2020). A first look at cloud inhomogeneity and its effect on  
502 lightning optical emission. *Geophysical Research Letters*, 47, e2020GL087094.  
503 <https://doi.org/10.1029/2020GL087094>
- 504 Bruning, E., Tillier, C. E., Edgington, S. F., Rudlosky, S. D., Zajic, J., Gravelle, C., et al. (2019).  
505 Meteorological imagery for the geostationary lightning mapper. *Journal of Geophysical*  
506 *Research: Atmospheres*, 2019; 124: 14285– 14309.  
507 <https://doi.org/10.1029/2019JD030874>
- 508 Christian, H. J., R. J. Blakeslee, S. J. Goodman, and D. M. Mach (Eds.), (2000). Algorithm  
509 Theoretical Basis Document (ATBD) for the Lightning Imaging Sensor (LIS),  
510 NASA/Marshall Space Flight Center, Alabama. (Available as  
511 <http://eosps0.gsfc.nasa.gov/atbd/listables.html>, posted 1 Feb. 2000).
- 512 Goodman, S. J., R. J. Blakeslee, W. J. Koshak, D. Mach, J. Bailey, D. Buechler, L. Carey, C.  
513 Schultz, M. Bateman, E. McCaul Jr., and G. Stano, (2013). The GOES-R geostationary  
514 lightning mapper (GLM). *J. Atmos. Res.*, **125-126**, 34-49
- 515 Hutchins, M. L., Holzworth, R. H., Brundell, J. B., and Rodger, C. J. ( 2012), Relative detection  
516 efficiency of the World Wide Lightning Location Network, *Radio Sci.*, 47, RS6005,  
517 doi:[10.1029/2012RS005049](https://doi.org/10.1029/2012RS005049).
- 518 Jacobson, A.R., R. Holzworth, J. Harlin, R. Dowden, and E. Lay, 2006: Performance Assessment  
519 of the World Wide Lightning Location Network (WWLLN), Using the Los Alamos  
520 Sferic Array (LASA) as Ground Truth. *J. Atmos. Oceanic Technol.*, **23**, 1082–1092,  
521 <https://doi.org/10.1175/JTECH1902.1>
- 522 Jacobson, A. R., & Light, T. E. L. (2012). Revisiting" Narrow Bipolar Event" intracloud  
523 lightning using the FORTE satellite. In *Annales Geophysicae* (Vol. 30, No. 2, p. 389).  
524 Copernicus GmbH.
- 525 Koshak, W. J., Solakiewicz, R. J., Phanord, D. D., and Blakeslee, R. J. ( 1994), Diffusion model  
526 for lightning radiative transfer, *J. Geophys. Res.*, 99( D7), 14361– 14371,  
527 doi:[10.1029/94JD00022](https://doi.org/10.1029/94JD00022).
- 528 Koshak, W. J. (2010). Optical Characteristics of OTD Flashes and the Implications for Flash-  
529 Type Discrimination, *Journal of Atmospheric and Oceanic Technology*, 27(11), 1822-  
530 1838. Retrieved Jan 21, 2021, from  
531 [https://journals.ametsoc.org/view/journals/atot/27/11/2010jtecha1405\\_1.xml](https://journals.ametsoc.org/view/journals/atot/27/11/2010jtecha1405_1.xml)
- 532 Lang, T. J., Pédeboy, S., Rison, W., Cervený, R. S., Montanyà, J., Chauzy, S., ... & Krahenbuhl,  
533 D. S. (2017). WMO world record lightning extremes: Longest reported flash distance and  
534 longest reported flash duration. *Bulletin of the American Meteorological Society*, 98(6),  
535 1153-1168.
- 536 Lay, E. H., Holzworth, R. H., Rodger, C. J., Thomas, J. N., Pinto, O., and Dowden, R. L. (2004),  
537 WWLL global lightning detection system: Regional validation study in Brazil, *Geophys.*  
538 *Res. Lett.*, 31, L03102, doi:[10.1029/2003GL018882](https://doi.org/10.1029/2003GL018882).
- 539 Light, T. E., Suszcynsky, D. M., and Jacobson, A. R. ( 2001a), Coincident radio frequency and

- 540 optical emissions from lightning, observed with the FORTE satellite, *J. Geophys. Res.*,  
 541 106( D22), 28223– 28231, doi:[10.1029/2001JD000727](https://doi.org/10.1029/2001JD000727).
- 542 Light, T. E., Suszcynsky, D. M., Kirkland, M. W., and Jacobson, A. R. ( 2001b), Simulations of  
 543 lightning optical waveforms as seen through clouds by satellites, *J. Geophys. Res.*, 106(  
 544 D15), 17103– 17114, doi:[10.1029/2001JD900051](https://doi.org/10.1029/2001JD900051).
- 545 Mach, D. M. (2020). Geostationary Lightning Mapper clustering algorithm stability. *Journal of*  
 546 *Geophysical Research: Atmospheres*, 125, e2019JD031900.  
 547 <https://doi.org/10.1029/2019JD031900>.
- 548 Peterson, M. (2019a). Using lightning flashes to image thunderclouds. *Journal of Geophysical*  
 549 *Research: Atmospheres*, 124, 10175– 10185. <https://doi.org/10.1029/2019JD031055>
- 550 Peterson, M. (2019b). Research applications for the Geostationary Lightning Mapper operational  
 551 lightning flash data product. *Journal of Geophysical Research: Atmospheres*, 124,  
 552 10205– 10231. <https://doi.org/10.1029/2019JD031054>
- 553 Peterson, M. (2020a). Modeling the transmission of optical lightning signals through complex 3-  
 554 D cloud scenes. *Journal of Geophysical Research: Atmospheres*, 125, e2020JD033231.  
 555 <https://doi.org/10.1029/2020JD033231>
- 556 Peterson, M. (2020b). Holes in Optical Lightning Flashes: Identifying Poorly-Transmissive  
 557 Clouds in Lightning Imager Data. *Earth and Space Science*, 7,  
 558 e2020EA001294<https://doi.org/10.1029/2020EA001294>
- 559 Peterson, M. (2020c). Removing solar artifacts from Geostationary Lightning Mapper data to  
 560 document lightning extremes. *Journal of Applied Remote Sensing*, 14(3), 032402.
- 561 Peterson, M. (2021a). GLM-CIERRA <http://dx.doi.org/10.5067/GLM/CIERRA/DATA101>
- 562 Peterson, M. (2021b). Coincident Optical and RF Lightning Detections from a Colombia  
 563 Thunderstorm. <https://doi.org/10.7910/DVN/5FR6JB>, Harvard Dataverse, V1
- 564 Peterson, M., & Lay, E. (2020). GLM observations of the brightest lightning in the Americas.  
 565 *Journal of Geophysical Research: Atmospheres*, 125, e2020JD033378. Peterson, M. J.,  
 566 Lang, T. J., Bruning, E. C., Albrecht, R., Blakeslee, R. J., Lyons, W. A., et al. (2020a).  
 567 New World Meteorological Organization certified megafash lightning extremes for flash  
 568 distance (709 km) and duration (16.73 s) recorded from space. *Geophysical Research*  
 569 *Letters*, 47, e2020GL088888. <https://doi.org/10.1029/2020GL088888>
- 570 Peterson, M., Rudlosky, S., & Deierling, W. (2017). The evolution and structure of extreme  
 571 optical lightning flashes. *Journal of Geophysical Research: Atmospheres*, 122, 13,370–  
 572 13,386. <https://doi.org/10.1002/2017JD026855>
- 573 Peterson, M., Rudlosky, S., & Deierling, W. (2018). Mapping the lateral development of  
 574 lightning flashes from orbit. *Journal of Geophysical Research: Atmospheres*, 123, 9674–  
 575 9687. <https://doi.org/10.1029/2018JD028583>
- 576 Peterson, M., Rudlosky, S., & Zhang, D. (2020b). Changes to the appearance of optical lightning  
 577 flashes observed from space according to thunderstorm organization and structure.  
 578 *Journal of Geophysical Research: Atmospheres*, 125, e2019JD031087.  
 579 <https://doi.org/10.1029/2019JD031087>
- 580 Peterson, M., Light, T., & Mach, D. (2021a). The Illumination of Thunderclouds by Lightning:  
 581 Part 1: The Extent and Altitude of Optical Lightning Sources. *Journal of Geophysical*  
 582 *Research: Atmospheres*.
- 583 Peterson, M., Light, T., & Mach, D. (2021b). The Illumination of Thunderclouds by Lightning:  
 584 Part 3: Retrieving Optical Source Altitude. *Journal of Geophysical Research:*  
 585 *Atmospheres*.

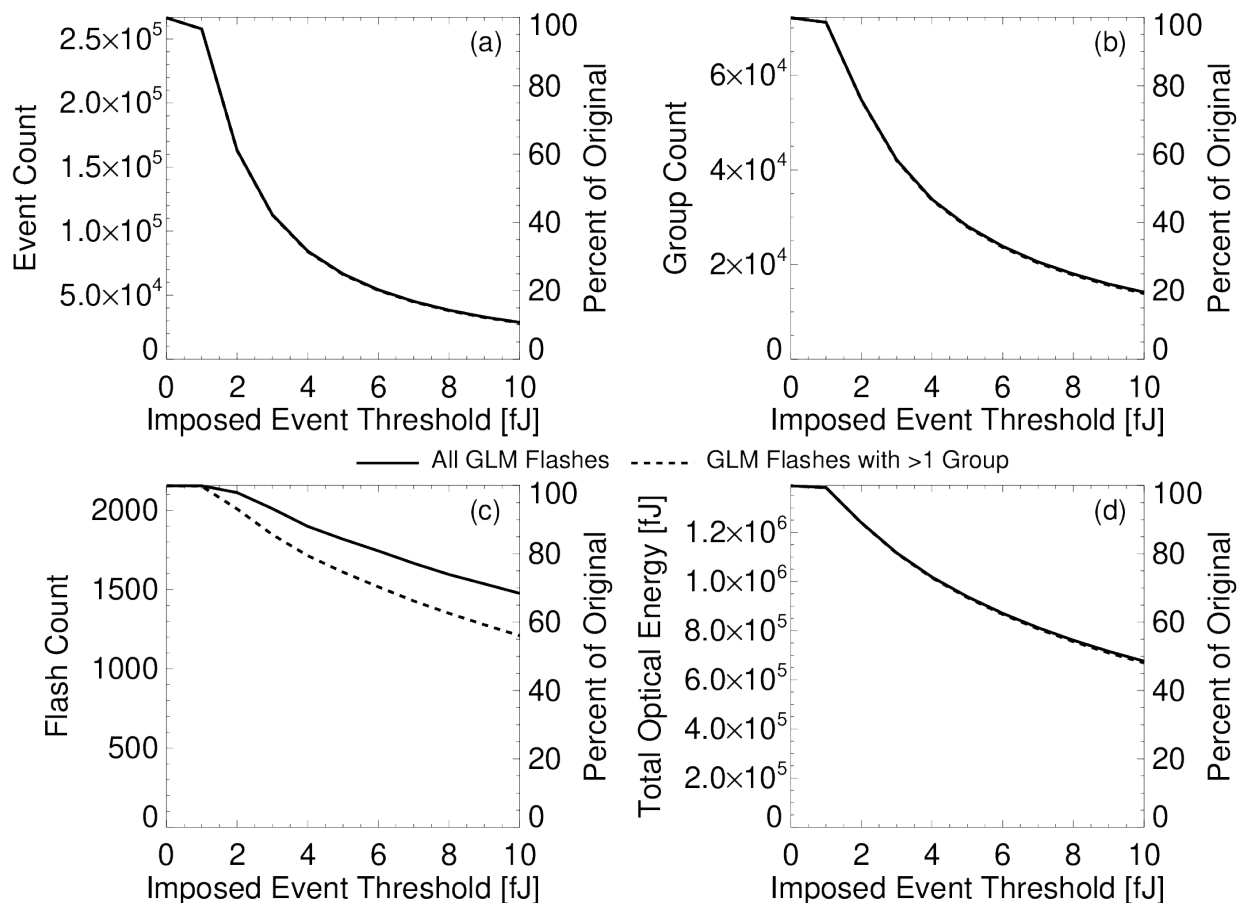
- 586 Peterson, M., & Mach, D. (2021c). The Illumination of Thunderclouds by Lightning: Part 4:  
 587 Volumetric Thunderstorm Imagery. *Journal of Geophysical Research: Atmospheres*.
- 588 Rison, W., Thomas, R. J., Krehbiel, P. R., Hamlin, T., & Harlin, J. (1999). A GPS-based three-  
 589 dimensional lightning mapping system: Initial observations in central New Mexico.  
 590 *Geophysical research letters*, 26(23), 3573-3576.
- 591 Rudlosky, S. D., S. J. Goodman, K. S. Virts, and E. C. Bruning, (2019). Initial geostationary  
 592 lightning mapper observations. *Geophys. Res. Lett.*, **46**, 1097– 1104.  
 593 <https://doi.org/10.1029/2018GL081052>
- 594 Rudlosky, S. D. and K. S. Virts, (2021). Dual Geostationary Lightning Mapper Observations.  
 595 *Mo. Wea. Rev.*, 149, 979-998, <https://doi.org/10.1175/MWR-D-20-0242.1>.
- 596 Rutledge, S. A., K. Hilburn, A. Clayton, & B. Fuchs, (2019). CSU GLM work summary. *GLM*  
 597 *Science Team Meeting, 2019*. Huntsville, AL, USA, 20 slides. Available online at:  
 598 [https://goes-r.nsstc.nasa.gov/home/sites/default/files/2019-](https://goes-r.nsstc.nasa.gov/home/sites/default/files/2019-09/GLM%20presentation%20Sept%202019_FINAL.pptx)  
 599 [09/GLM%20presentation%20Sept%202019\\_FINAL.pptx](https://goes-r.nsstc.nasa.gov/home/sites/default/files/2019-09/GLM%20presentation%20Sept%202019_FINAL.pptx).
- 600 Rodger, C. J., Werner, S., Brundell, J. B., Lay, E. H., Thomson, N. R., Holzworth, R. H., &  
 601 Dowden, R. L. (2006, December). Detection efficiency of the VLF World-Wide  
 602 Lightning Location Network (WLLN): initial case study. In *Annales Geophysicae*  
 603 (Vol. 24, No. 12, pp. 3197-3214). Copernicus GmbH.
- 604 Said, R., & M. Murphey, (2019). Spatiotemporal patterns of GLM flash DE. *GLM Science Team*  
 605 *Meeting, 2019*. Huntsville, AL, USA, 18 slides. Available online at: [https://goes-](https://goes-r.nsstc.nasa.gov/home/sites/default/files/2019-09/Said_GLM_2019.pptx)  
 606 [r.nsstc.nasa.gov/home/sites/default/files/2019-09/Said\\_GLM\\_2019.pptx](https://goes-r.nsstc.nasa.gov/home/sites/default/files/2019-09/Said_GLM_2019.pptx).
- 607 Thomas, R., (2019). Low GLM detection efficiencies in large storms. *GLM Science Team*  
 608 *Meeting, 2019*. Huntsville, AL, USA, 18 slides. Available online at: [https://goes-](https://goes-r.nsstc.nasa.gov/home/sites/default/files/2019-09/Thomas-GLM-sci-meeting-2019.pdf)  
 609 [r.nsstc.nasa.gov/home/sites/default/files/2019-09/Thomas-GLM-sci-meeting-2019.pdf](https://goes-r.nsstc.nasa.gov/home/sites/default/files/2019-09/Thomas-GLM-sci-meeting-2019.pdf).
- 610 Thomson, L.W. and E.P. Krider, (1982). The Effects of Clouds on the Light Produced by  
 611 Lightning. *J. Atmos. Sci.*, **39**, 2051–2065, [https://doi.org/10.1175/1520-](https://doi.org/10.1175/1520-0469(1982)039<2051:TEOCOT>2.0.CO;2)  
 612 [0469\(1982\)039<2051:TEOCOT>2.0.CO;2](https://doi.org/10.1175/1520-0469(1982)039<2051:TEOCOT>2.0.CO;2)
- 613 [van der Velde, O. A., Montanya, J., Neubert, T., Chanrion, O., Østgaard, N., Goodman, S., et al.](https://doi.org/10.1029/2020EA001249)  
 614 [\(2020\). Comparison of high-speed optical observations of a lightning flash from space](https://doi.org/10.1029/2020EA001249)  
 615 [and the ground. \*Earth and Space Science\*, 7, e2020EA001249.](https://doi.org/10.1029/2020EA001249)  
 616 <https://doi.org/10.1029/2020EA001249>
- 617 Zhu, Y., Rakov, V. A., Tran, M. D., Stock, M. G., Heckman, S., Liu, C., ... Hare, B. M. ( 2017).  
 618 Evaluation of ENTLN performance characteristics based on the ground truth natural and  
 619 rocket-triggered lightning data acquired in Florida. *Journal of Geophysical Research:*  
 620 *Atmospheres*, 122. 9858– 9866, <https://doi.org/10.1002/2017JD027270>

621  
 622  
 623



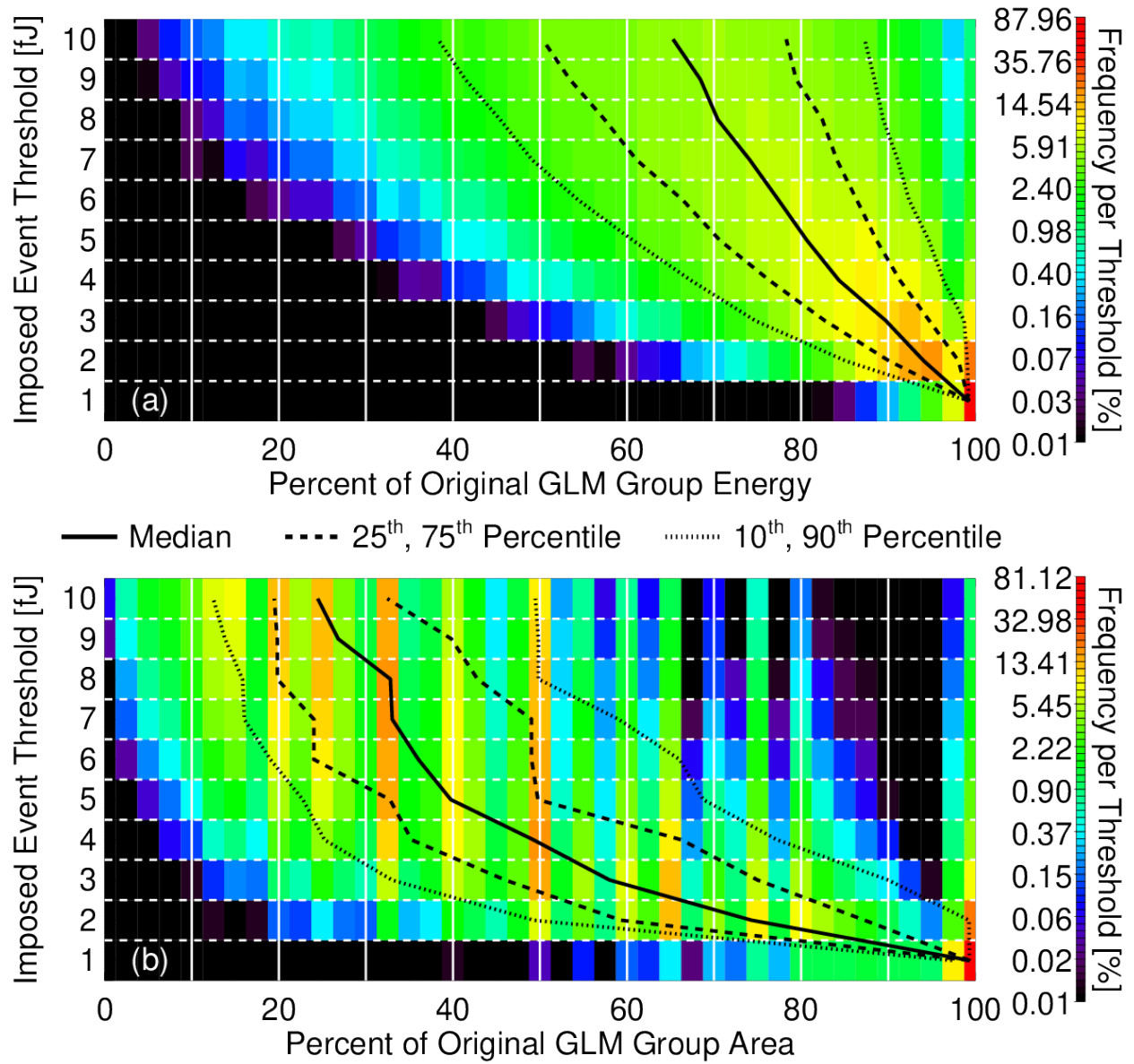
624  
 625  
 626  
 627  
 628  
 629  
 630  
 631  
 632  
 633

**Figure 1.** Timeseries of GLM minimum event energy during a thunderstorm over (a) Colombia near the satellite subpoint where thresholds are generally low and (b) Colorado where thresholds are known to be relatively high. Minimum event energies are computed for every pixel and the minimum (red), mean (dark blue) and maximum (light blue) values over each region are reported.

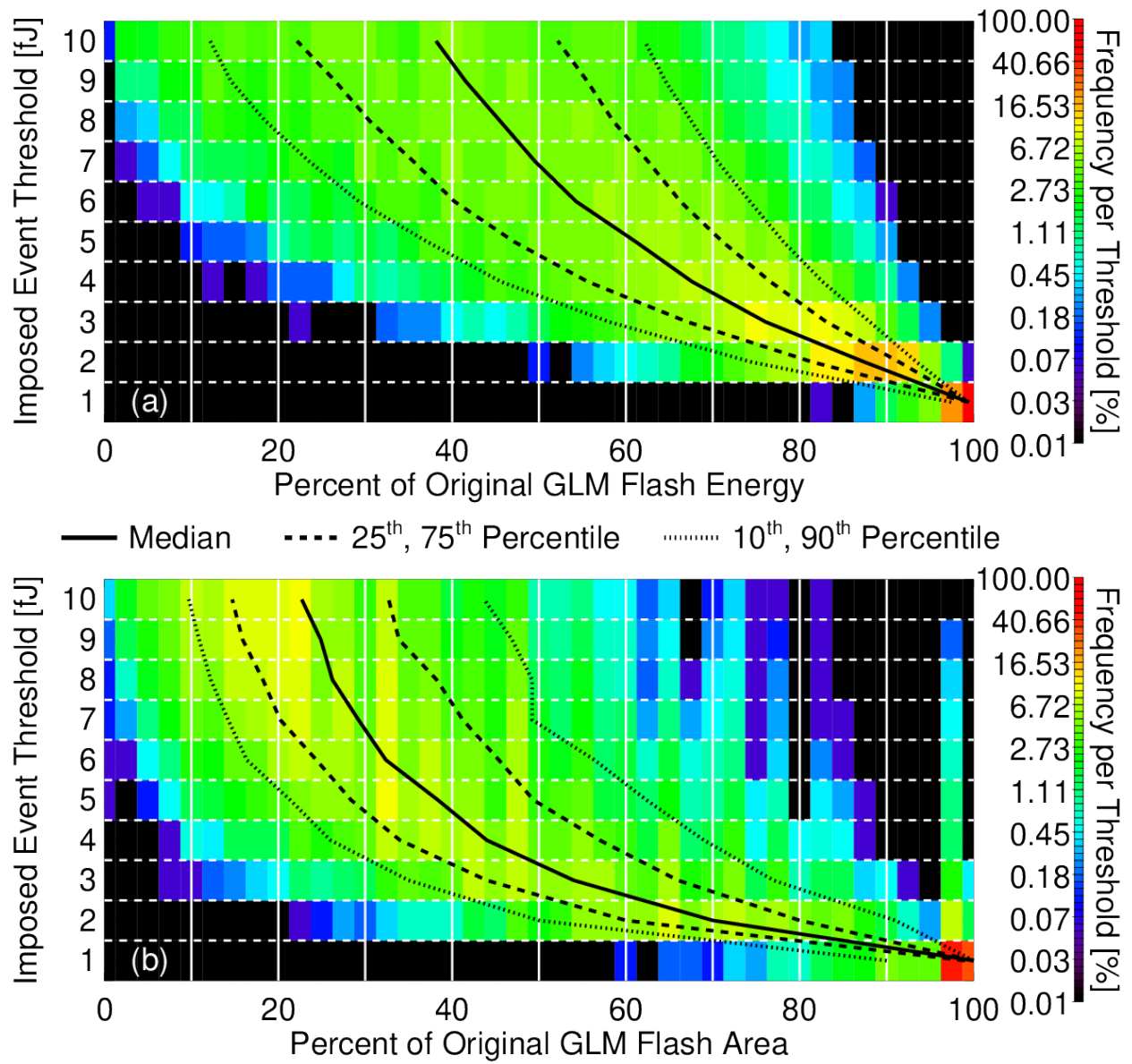


634  
635  
636  
637  
638  
639  
640

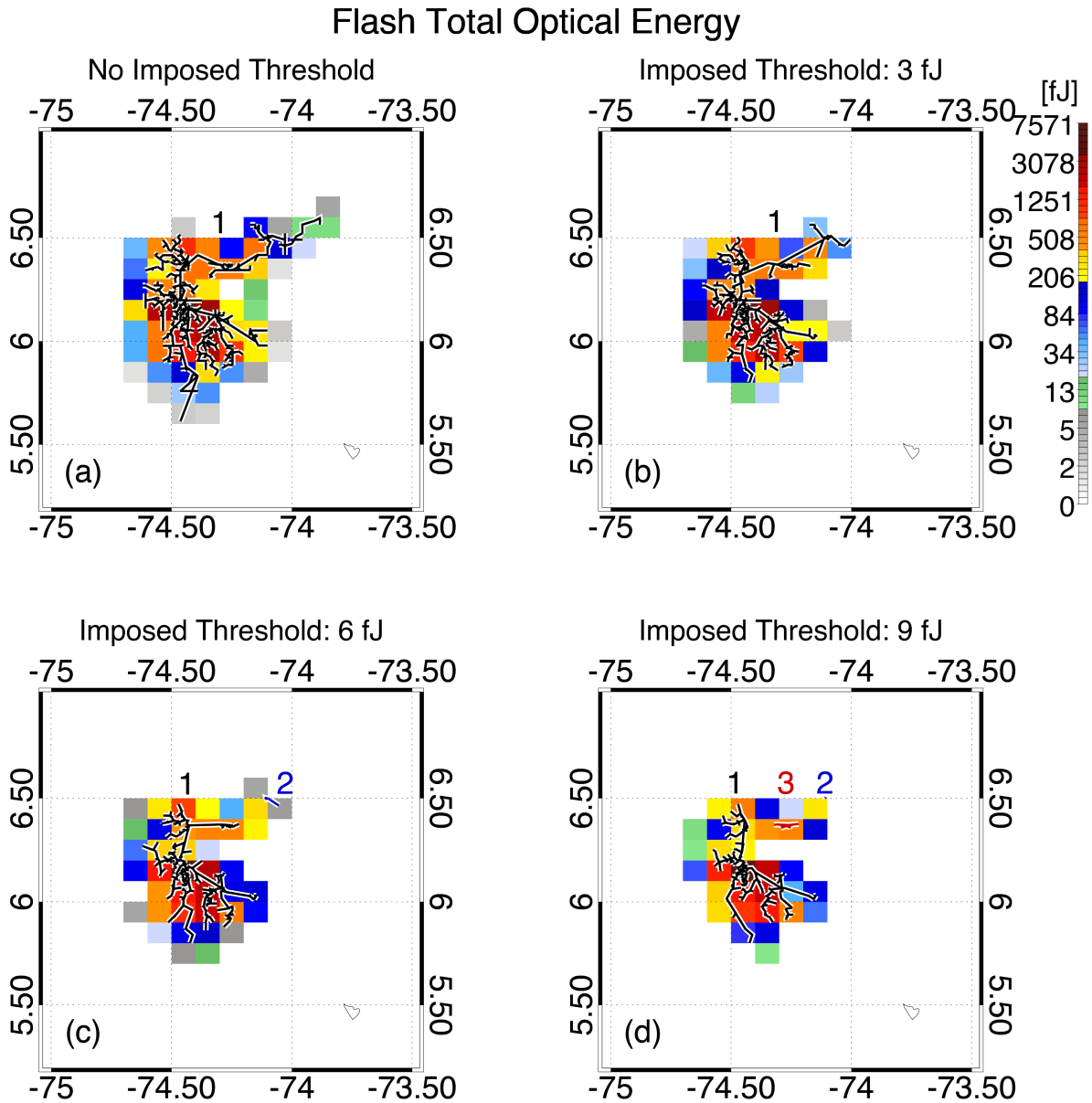
**Figure 2.** GLM (a) event, (b) group, and (c) flash counts, and (d) Total Optical Energies from the Colombia thunderstorm under artificial thresholds ranging from 0 fJ (original instrument thresholds) to 10 fJ. Solid curves indicate all GLM flashes while dashed curves only consider multi-group flashes that would not be removed by the LCFA.



641  
 642 **Figure 3.** Histograms of GLM (a) group energy and (b) group area under each imposed  
 643 threshold. Only groups whose maximum event energies exceed 10 fJ are considered.  
 644

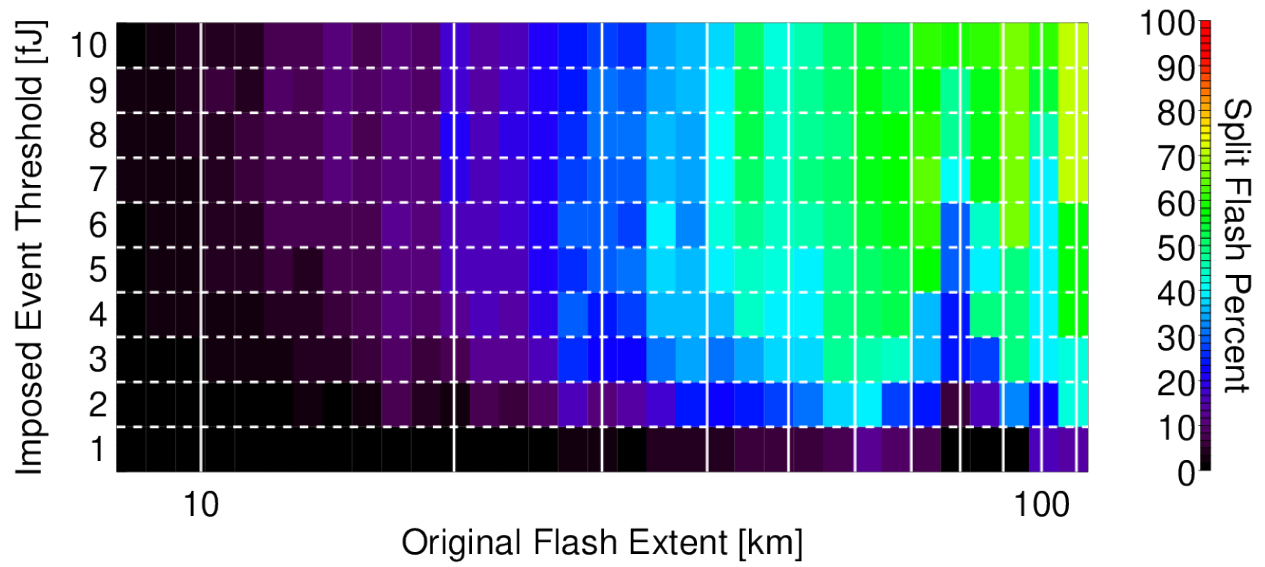


645  
 646 **Figure 4.** As in Figure 3, but for GLM flashes rather than groups.  
 647

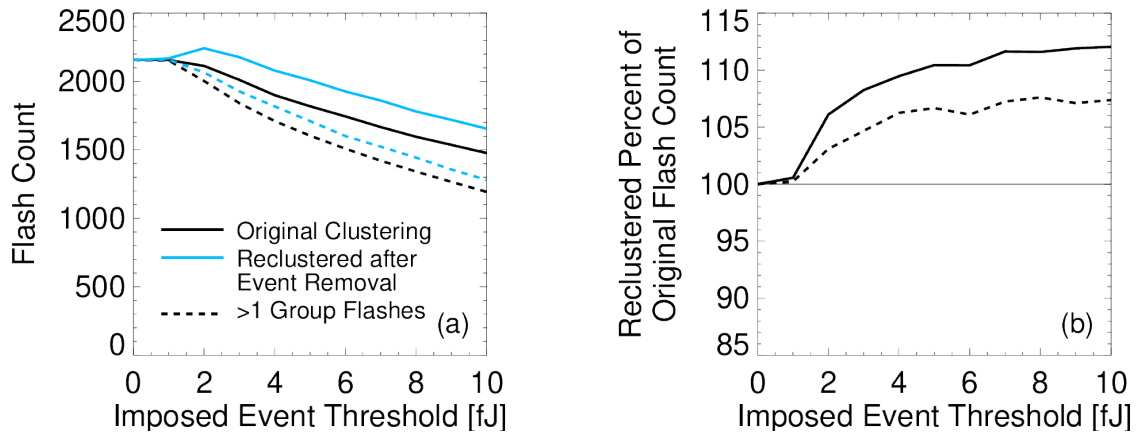


648  
649

650 **Figure 5.** GLM total optical energies (color contour) and progression of groups over time (line  
651 segments) from a long horizontal lightning flash under (a) no imposed threshold, (b) a 3 fJ  
652 threshold, (c) a 6 fJ threshold, and (d) a 9 fJ threshold. Flash sections that are split at higher  
653 thresholds are indicated as disconnected line segments with a unique color and listed index for  
654 each split flash.  
655

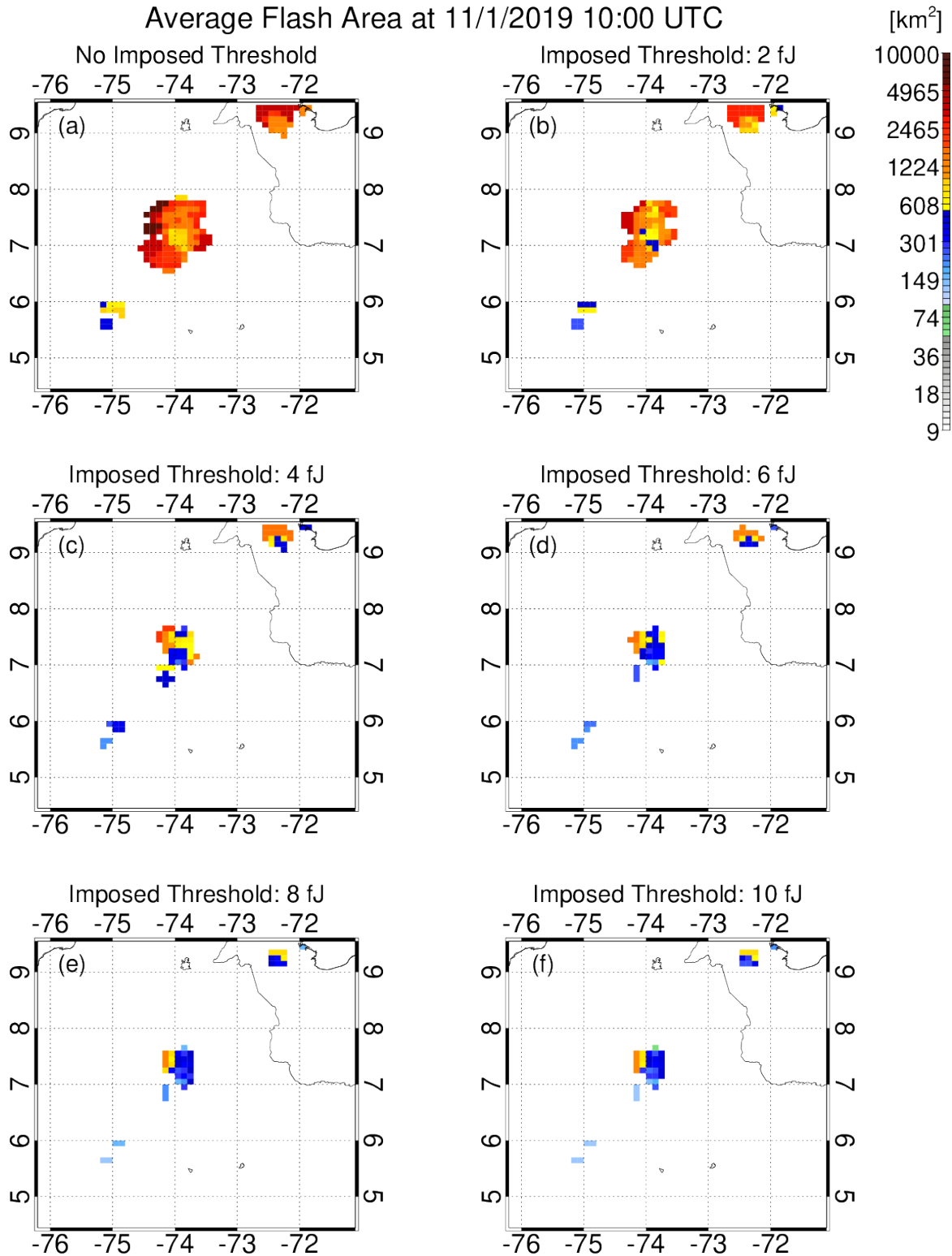


656  
657 **Figure 6.** Fractions of flashes that become split after imposing an artificial threshold categorized  
658 by original flash extent.  
659



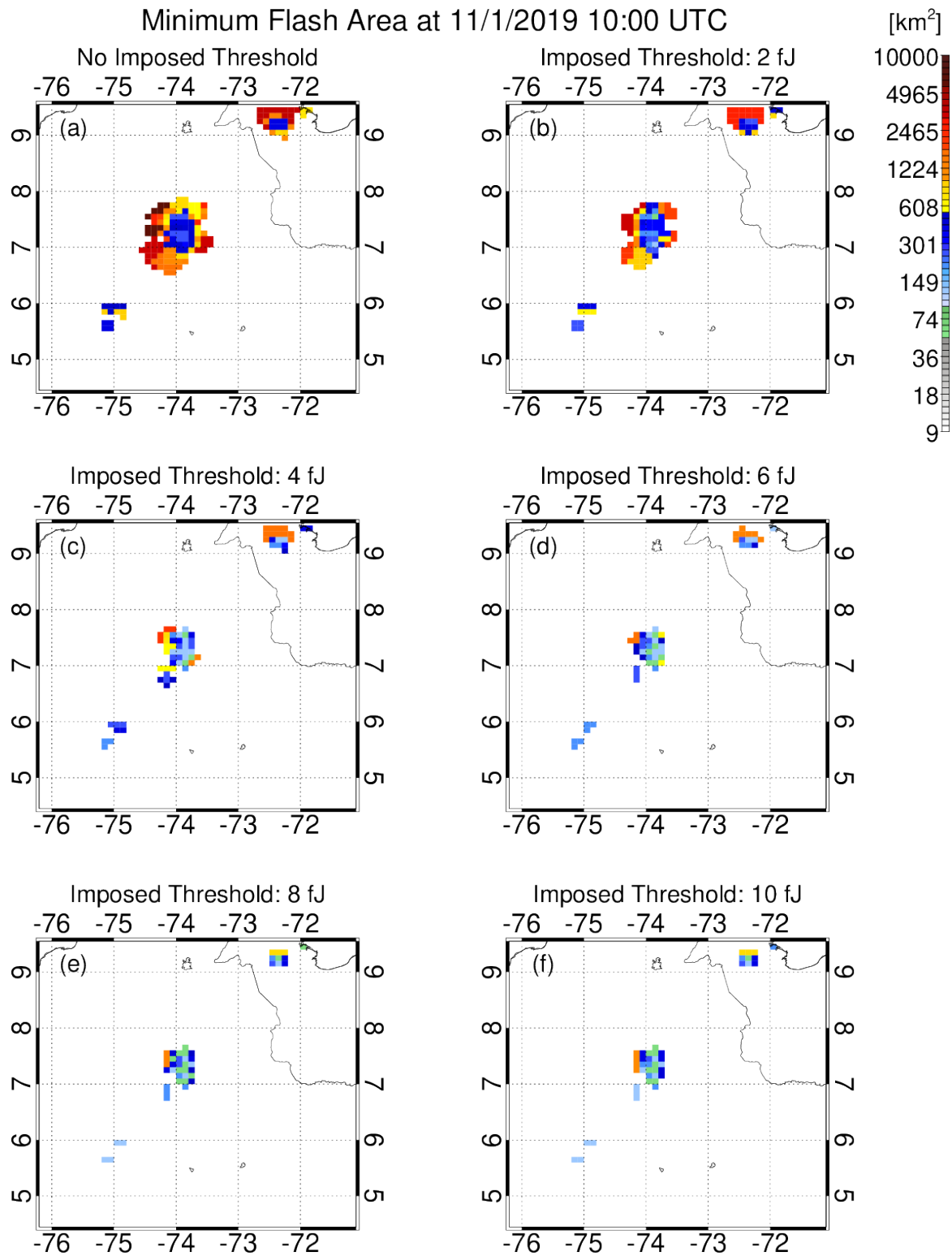
660  
661  
662  
663  
664  
665  
666

**Figure 7.** The effect of flash splitting on flash rates. (a) The total number of original flashes (black) and flashes that have been reclustered to account for splitting (blue) at each imposed threshold. (b) The ratio of reclustered flashes to the original flash count at each threshold. Solid lines include all flashes while dashed lines only consider multi-group flashes.



667  
668  
669  
670  
671

**Figure 8.** Average Flash Area (AFA) grids generated from (a) the original GLM data and the reclustered data under artificial thresholds of (b) 2 fJ, (c) 4 fJ, (d) 6 fJ, (e) 8 fJ, and (f) 10 fJ.



672  
673  
674

**Figure 9.** As in Figure 8, but for Minimum Flash Area (MFA) grids.